PHYSICAL REVIEW A **85**, 020701(R) (2012)

Selective production of the doubly excited $2p^2$ (^1D) state in He-like Ar^{16+} ions by resonant coherent excitation

Y. Nakano,[1,2,*] S. Suda,[1,2] A. Hatakeyama,[3] Y. Nakai,[4] K. Komaki,[1,5] E. Takada,[6] T. Murakami,[6] and T. Azuma[1,2]

[1]*RIKEN Advanced Science Institute, Wako, Saitama 351-0198, Japan*

[2]*Department of Physics, Tokyo Metropolitan University, Hachioji, Tokyo 192-0397, Japan*

[3]*Department of Applied Physics, Tokyo University of Agriculture and Technology, Koganei, Tokyo 184-8588, Japan*

[4]*RIKEN Nishina Center, Wako, Saitama 351-0198, Japan*

[5]*Graduate School of Arts and Sciences, University of Tokyo, Komaba, Meguro, Tokyo 153-8902, Japan*

[6]*National Institute of Radiological Sciences, Inage, Chiba 263-8555, Japan*

(Received 11 April 2011; revised manuscript received 17 November 2011; published 3 February 2012)

Selective production of the doubly excited state in 464 MeV/u He-like Ar^{16+} ions was accomplished using three-dimensional resonant coherent excitation in a thin foil of silicon crystal. Through a coherent interaction with the periodic crystal field, the Ar^{16+} ions were resonantly excited sequentially from the ground state to the $1s2p$ (^1P) state and then $2p^2$ (^1D) state in a way analogous to two-color x-ray laser excitation. The periodic crystal fields of 10^{11} V/m in the projectile's frame are equivalent to the fields generated by x-ray lasers with photon energies of 3139.55 and 3286.95 eV and an energy flux of 10^{16} W/cm^2. We confirmed the doubly excited state formation through observation of the subsequent collisional ionization, Auger ionization, and radiative deexcitation.

DOI: 10.1103/PhysRevA.85.020701 PACS number(s): 34.50.Fa, 32.80.Hd, 61.85.+p

Multiply excited states of few-electron atoms and ions have attracted our interest as an ideal object to investigate the dynamics of strongly-correlated bound electrons, which cannot be considered in an independent-particle picture. The simplest case among such systems is the doubly excited atomic helium [1], of which numerous photoexcitation spectroscopies have been performed using synchrotron radiation [2,3]. An isoelectronic study of such an He-like system would reveal the quantum kinematics of strongly correlated three-body systems under the relativistic and quantum electrodynamic (QED) effects, however, the synchrotron radiation is not applicable to He-like high-Z ions because of their limited wavelength and intensities. So far the production of doubly excited He-like ions in the high-Z region can be realized exclusively by electron capture of H-like ions during collisions with target atoms or electron beams, i.e., the resonant transfer and excitation [4,5] or the dielectronic recombination [6], respectively. Although these methods were quite successful in determining their binding energies, their decay processes after the production have not been studied particularly because such collision experiments often suffer from unexpected inelastic collision processes, as well as the difficulties in observing all of the decay channels. On the other hand, the information about the dynamic behavior of correlated electrons is offered by an investigation of their decay dynamics. For these studies, instead of using collision processes, a new approach is needed to produce the doubly excited states in a selective and well-controlled manner within a short interaction time. Such a refined population manipulation is achieved only in alkaline-earth-metal atoms by a laser double-excitation technique [7], in which two valence electrons are both excited by polarization-controlled laser fields. Although the advancing x-ray free-electron lasers are powerful tools in atomic physics in the x-ray domain, the two-color population control in few-electron high-Z ions is still not achieved.

In this Rapid Communication, we demonstrate an alternative approach to realize a coherent excitation of He-like high-Z ions from their ground state to a specific doubly excited states. This scheme is an analogy of the laser double excitation in the x-ray domain, but we used a resonant coherent excitation (RCE) instead of the laser excitation. The RCE of heavy ions can occur when they penetrate a thin crystalline target at a relativistic velocity [12]. As they travel, the spatially periodic Coulomb potential in the target crystal acts on them as a rapidly oscillating electric field at an x-ray frequency domain. From the Fourier potential of the crystal, the amplitude of oscillating crystal fields is derived to be 10^{11} V/m in the rest frame of projectiles (P frame), which is equivalent to that generated by a laser field of 10^{16} W/cm^2. Since the first experimental observation by Datz *et al.* in 1978 [13], the dynamics of the RCE process has been extensively studied under the axial and planar channeling conditions. On the other hand, recently we demonstrated a different type of RCE, i.e., the three-dimensional RCE (3D-RCE) [14], which does not require the channeling conditions. This discovery of the 3D-RCE added two features to the existing RCE method that enabled the double resonance and polarization control techniques [15,16]. As such, the 3D-RCE comes to be expected as a versatile tool in the population manipulation of high-Z ions in the x-ray domain. In the present study, we made the first attempt to perform a double x-ray experiment to manipulate two electrons of He-like ions. The double-excitation scheme was applied to a He-like Ar^{16+} ion in a ladder-type configuration, as illustrated in Fig. 1, to selectively populate the $2p^2$ (^1D) state. The required excitation energies for the first and second transitions were $\Delta E_1 = 3139.55$ eV and $\Delta E_2 = 3286.95$ eV, respectively [8].

The experiment was performed at the National Institute of Radiological Sciences (NIRS), Japan. A beam of

*nakano-y@riken.jp

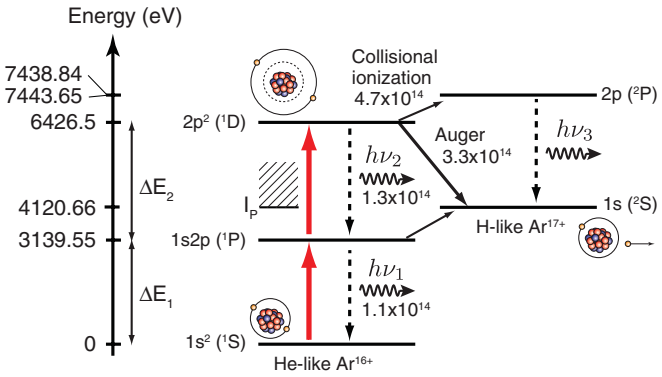

FIG. 1. (Color) Energy levels of He-like Ar^{16+} and H-like Ar^{17+} [8] with their rates (in s^{-1}) for radiative deexcitation [9], collisional ionization [10], and the Auger ionization [11].

464.12 MeV/u He-like Ar^{16+} ions with a small divergence of 0.04 mrad was provided by the Heavy Ion Medical Accelerator in Chiba (HIMAC). The schematic layout of the setup is shown in Fig. 2(a). We observed the ionization process of the ions in a 1-μm-thick Si crystal by detecting the released electrons as well as the final charge-state distribution of the ions. The inset of Fig. 2(a) shows the geometrical configuration of a small magnetic analyzer ($\sim$10 mT) for electrons. The electrons were deflected by 90° in the analyzer and detected using a 450-μm-thick silicon solid-state detector (SSD) through a pair of ϕ3 mm apertures, which were separated by 95 mm. The geometrical acceptance angles of the analyzer were 1° and 0.4° for the horizontal and vertical directions, respectively. The transmitted ions were charge separated by another dipole magnet ($\sim$0.5 T) at 1.2 m downstream of the target crystal and detected with a 2D position-sensitive detector (2D-PSD). The deexcitation radiations from the excited ions were observed using a Si(Li) x-ray detector with a detection area of 30 mm^2, which was installed at a distance of 180 mm and at 41° from the beam within the same horizontal plane as the beam. The target crystal was mounted on a three-axis, high-precision goniometer, which manipulated the rotation angle θ and tilt angle ϕ of the crystal relative to the ion beam. The origin of these angles was set such that the $[\bar{1}10]$ axis coincides with the beam axis, and the (220) plane is horizontal. In this case, if we redefine the base vectors for the reciprocal lattice space as $([\bar{1}10]/a,[001]/a,[110]/a)$ (a is the lattice constant), the frequency of the oscillating crystal field in the P frame is given as

$$\nu_{klm}(\theta,\phi) = \frac{\gamma\beta c}{a}\{\sqrt{2}(k\cos\phi + m\sin\phi)\cos\theta + l\sin\theta\}, \quad (1)$$

where $\gamma = (1-\beta^2)^{-1/2}$ is the Lorentz factor, $\beta = v/c$ (v is the ion velocity and c is the light velocity), and (k,l,m) are the Miller indices [14]. The resonance condition for the RCE of transition energy ΔE is satisfied when $h\nu_{klm}(\theta,\phi) = \Delta E$, where h is the Planck's constant. In Fig. 2(b), the blue and red lines represent the angular conditions satisfying $h\nu_{1,-2,-3}(\theta,\phi) = \Delta E_1$ and $h\nu_{1,-1,2}(\theta,\phi) = \Delta E_2$, respectively. These two lines cross each other at $(\theta,\phi) = (5.73, -0.34)$, where the RCE conditions for both transitions are satisfied simultaneously, i.e., the double-resonance (DR) condition is satisfied. On the other hand, we set the incident

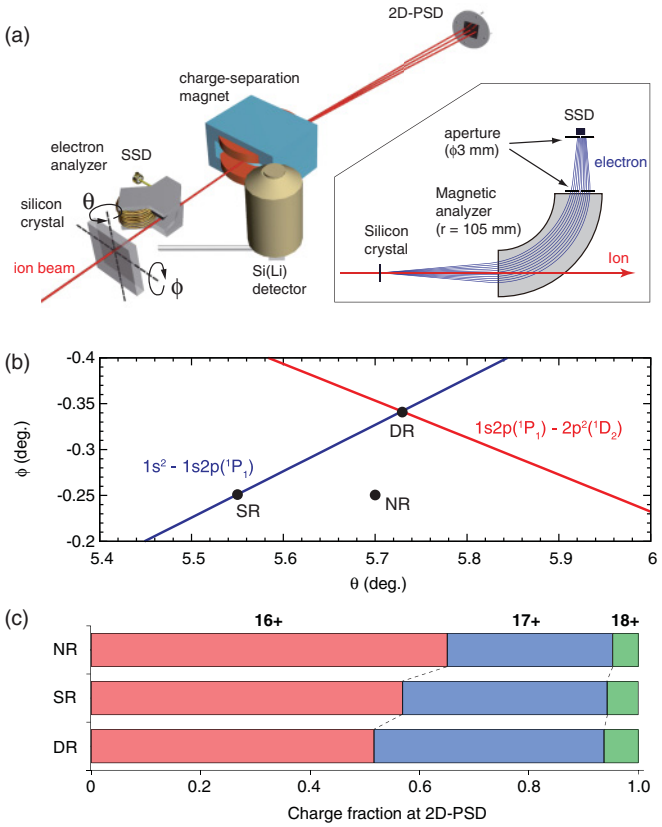

FIG. 2. (Color) (a) Schematic layout of the experimental setup and detailed geometry of the electron analyzer. (b) The resonance conditions for RCE of $1s^2 - 1s2p$ (blue line) and $1s2p - 2p^2$ (red line), respectively. The dots are the conditions used in the measurements for the NR, SR, and DR conditions. (c) The charge-state distribution of transmitted Ar ions at the 2D-PSD observed under the NR, SR, and DR conditions.

angles to $(\theta,\phi) = (5.55, -0.25)$ for the single resonance (SR) condition of the lower transition $(1s^2 - 1s2p)$, and $(5.70, -0.25)$ for the nonresonance (NR) condition.

Figure 2(c) shows the final charge-state distribution of the transmitted ions observed with the 2D-PSD. In this relativistic collision energy, cross sections of the projectile's electron-capture process in the target crystal are negligibly small. Ionization cross sections are also reduced significantly. As a result, 63% of the incident Ar^{16+} ions passed through the crystal without changing their charge state under the NR condition. However, this survival fraction of Ar^{16+} ions shows a decrease under the SR condition, because the ions excited to the $1s2p$ state in the crystal have a larger cross section for collisional ionization compared with the ground-state ions. Under the DR condition, the survival fraction was even smaller than that under the SR condition. From the final charge-state distributions, the numbers of emitted electrons were found to be 0.49 and 0.54 per projectile ion under the SR and DR conditions, respectively. This enhancement of the electron emission under the DR condition can be attributed to both collisional ionization and Auger ionization of the $2p^2$ state.

To distinguish these two ionization processes, we observed the electron spectrum at 0° with respect to the ion beam. Figure 3(a) shows a 2D energy-momentum distribution of the

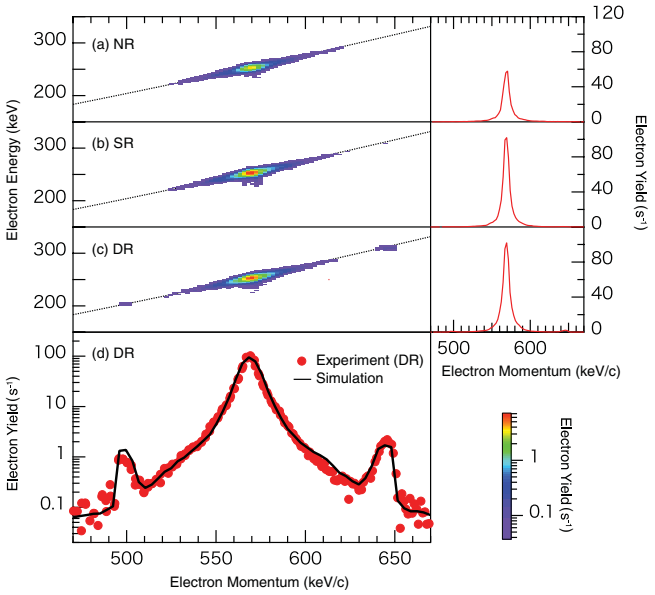

FIG. 3. (Color) Energy-momentum distribution of the observed electrons under the (a) NR, (b) SR, and (c) DR conditions. The dashed line represents the theoretical dispersion relationship of the electron energy and momentum. The projections onto the momentum axis, i.e., the electron-momentum spectra, are shown in a linear scale at the right side of the contour maps. The electron-momentum spectrum under the DR condition is also shown in a logarithmic scale in (d) with a result of Monte Carlo simulation. The electron yields are corrected against fluctuation of the beam intensity.

zero-degree electrons under the NR condition as a contour map. The x and y axes represent the electron momentum and energy, which are derived from the magnetic field of the analyzer and the energy deposition to the SSD, respectively. At the right side of the contour map, its projection onto the momentum axis is shown in a linear scale. The momentum spectrum exhibits a cusp-shaped distribution centered at the same velocity as the projectile beam, which are the so-called convoy electrons. In general, in zero-degree electron spectroscopies at MeV/u collision energies, the convoy electrons originate from both projectile and target ionization, i.e., the electron loss to continuum (ELC) and electron capture to continuum (ECC) [17–19]. In addition, the cusp peak is often superimposed by numerous peaks of Auger electrons from projectiles [20,21]. In the present case, the observed electrons are purely from the ELC process, because the cross sections for producing ECC electrons and Auger electrons are negligibly small in this relativistic collision. This allows a rigorous understanding of their atomic processes in the target crystal. Figures 3(b) and 3(c) are the same as 3(a), but obtained under the SR and DR conditions, respectively. Reflecting the increased ionization probability of the excited Ar^{16+} ions observed in Fig. 2(c), the convoy electron yield under the SR condition was enhanced from that under the NR condition. However, under the DR condition, we did not observe additional enhancement of the convoy electron yield from the SR condition, but two additional islands at each side of the cusp shape in the contour map. These equally separated two peaks represent the zero-degree Auger electrons emitted forward and backward from the projectile ions. Since the

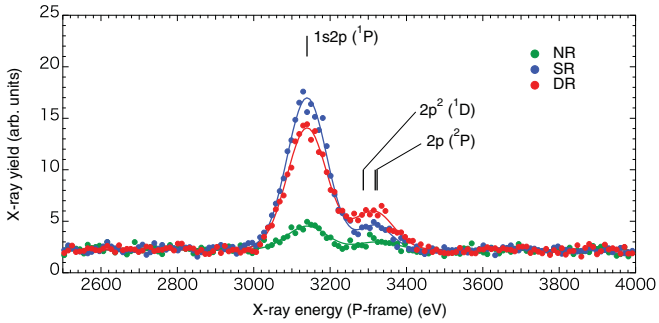

FIG. 4. (Color) P frame x-ray spectra emitted from the projectile ions under the NR, SR, and DR conditions. Two-component Gaussian curves are fitted to the spectra and are shown as solid lines to guide the eye.

ionization potential of the Ar^{16+} ion is $I_p = 4120.658$ eV [8], the Auger electron from the resonantly produced $2p^2$ (^1D) state has a kinetic energy of $\Delta E_1 + \Delta E_2 - I_p = 2305.84$ eV in the P frame. The energy loss and angular straggling of these electrons in the target is negligibly small. According to the Lorentz transformation, the momentum p of the zero-degree Auger electron in the laboratory frame (L frame) is given by $p = \gamma\gamma'_e m_e c(\beta \pm \beta'_e)$, where γ'_e and β'_e are the relativistic factors for the electron in the P frame. This yields 645.46 and 494.70 keV/c for the present Auger electron momenta emitted forward and backward, respectively, which agrees well with the observations.

Figure 3(d) shows the momentum spectrum of Fig. 3(c) in a logarithmic scale with a result of a Monte Carlo trajectory simulation. In the simulation, we calculated the classical trajectories of the electrons in the analyzer by considering the energy broadening, divergence, and spot size of the beam, as well as the effective fringing field of the magnetic analyzer. To reproduce the observed cusp-shaped peak in the L frame, we assumed a multiexponential momentum distribution of the ionized electrons in the P frame, in which the initial momentum distribution of the bound electrons [22] was not considered. For the Auger electrons, because the analyzer resolution is not enough to discuss their P frame angular distribution, we assumed an isotropic angular distribution for simplicity. The peak positions and the width of the Auger electrons in the simulation are in excellent agreement with those in the observed spectrum. From the relative yield of the Auger electrons to the convoy electrons, the number of emitted Auger electrons was estimated to be ~0.08 per incident ion. Considering the branching ratio of the Auger decay to other channels, this result suggests that more than 10% of the incident ions are excited to the $2p^2$ state under the DR condition. By comparison, if one estimates the mean population of the $2p^2$ state by a rate equation using cross sections from the ETACHA code [10], it would be less than 0.01.

The x-ray spectra observed with the Si(Li) detector are shown in Fig. 4 for the NR, SR, and DR conditions. The x axis was transformed from the L frame into the P frame energy. The left peak centered at 3139.55 eV represents the deexcitation x-ray emission from the $1s2p$ state. Under the NR condition, the x rays were emitted from the $1s2p$ state formed by the

collisional excitation in the target crystal. When a resonant condition is satisfied, the intensity of the $1s2p$ peak shows a significant enhancement. At the same time, a new peak appears at the right side of the $1s2p$ peak, which consists of the x-rays from the $2p$ and $2p^2$ states. Note that the production of the $2p$ or $2p^2$ state under the NR condition requires a two-step collision process, whose probability is negligibly small in this thin target. The right peak in the SR spectrum mainly originates from the deexcitation of the $2p$ state which was formed by a collisional ionization of the resonantly excited $1s2p$ state. Under the DR condition, the spectrum showed a decrease of the $1s2p$ peak simultaneously with an increase of the right peak. This represents the direct evidence of the population transfer from the $1s2p$ state to the $2p^2$ state induced under the DR condition. From the fitting of the $1s2p$ peak with a Gaussian function, this decrease in the intensity of the $1s2p$ peak was estimated to be about 20%. The increase in the right peak is attributed to the radiative decay of both the $2p^2$ and $2p$ states. The latter is explained by the collisional ionization of one electron in the $2p^2$ state followed by radiative decay of the other.

In summary, we successfully demonstrated the selective production of the doubly excited $2p^2$ (^1D) state through sequential 3D-RCEs of the ground-state Ar^{16+} ions in an efficient manner. The evidence was obtained from the observation of both Auger ionization and radiative deexcitation of the $2p^2$ state. Using a Monte Carlo simulation, the probability of the Auger electron emission was estimated to be as high as 8% under the DR condition. Considering the beam intensity of several million ions per second available at HIMAC, we could effectively excite more than 10^5 ions per second to the doubly excited state. We propose that this method would be a powerful tool for studying a series of correlated multibody quantum systems in high-Z ions. The use of a 2D position-sensitive electron detector combined with the polarization-control technique in 3D-RCE [16] will enable us to conduct a promising study of the angular distribution of Auger electrons from aligned states. The angular correlation between cascade radiations from these aligned doubly excited states as well as their branching ratio to Auger ionization are also of significant interest. In addition, an attempt to produce a triply excited state of Li-like Ar^{15+} ions is now underway.

This study was supported in part by Grants-in-Aid for Scientific Research (Grant No. 19104010) from the Japan Society for the Promotion of Science (JSPS). Y. Nakano acknowledges the support from JSPS (Grants No. 22840050 and No. 23740311). A.H. acknowledges support from the "Improvement of Research Environment for Young Researchers" program of MEXT. This experiment was one of the research projects with heavy ions at NIRS-HIMAC.

[1] G. Tanner, K. Richter, and J. M. Rost, Rev. Mod. Phys. **72**, 497 (2000).

[2] M. Domke, K. Schulz, G. Remmers, G. Kaindl, and D. Wintgen, Phys. Rev. A **53**, 1424 (1996).

[3] K. Schulz, G. Kaindl, M. Domke, J. D. Bozek, P. A. Heimann, A. S. Schlachter, and J. M. Rost, Phys. Rev. Lett. **77**, 3086 (1996).

[4] W. G. Graham, K. H. Berkner, E. M. Bernstein, M. W. Clark, B. Feinberg, M. A. McMahan, T. J. Morgan, W. Rathbun, A. S. Schlachter, and J. A. Tanis, Phys. Rev. Lett. **65**, 2773 (1990).

[5] X. Ma, P. H. Mokler, F. Bosch, A. Gumberidze, C. Kozhuharov, D. Liesen, D. Sierpowski, Z. Stachura, T. Stöhlker, and A. Warczak, Phys. Rev. A **68**, 042712 (2003).

[6] G. Kilgus, J. Berger, P. Blatt, M. Grieser, D. Habs, B. Hochadel, E. Jaeschke, D. Krämer, R. Neumann, G. Neureither *et al.*, Phys. Rev. Lett. **64**, 737 (1990).

[7] P. Camus, T. F. Gallagher, J. M. Lecomte, P. Pillet, L. Pruvost, and J. Boulmer, Phys. Rev. Lett. **62**, 2365 (1989).

[8] Yu. Ralchenko *et al.*, NIST Atomic Spectra Database Version 3.0 (2006) [http://physics.nist.gov/asd3].

[9] H. F. Beyer, H. J. Kluge, V. P. Shevelko, and H. J. Kluge, *X-Ray Radiation of Highly Charged Ions* (Springer-Verlag, Berlin, 1997).

[10] J. P. Rozet, C. Stéphan, and D. Vernhet, Nucl. Instrum. Methods Phys. Res. B **107**, 67 (1996).

[11] F. Koike (private communication).

[12] V. V. Okorokov, JETP Lett. **2**, 111 (1965).

[13] S. Datz, C. D. Moak, O. H. Crawford, H. F. Krause, P. F. Dittner, J. Gomez del Campo, J. A. Biggerstaff, P. D. Miller, P. Hvelplund, and H. Knudsen, Phys. Rev. Lett. **40**, 843 (1978).

[14] C. Kondo, S. Masugi, Y. Nakano, A. Hatakeyama, T. Azuma, K. Komaki, Y. Yamazaki, T. Murakami, and E. Takada, Phys. Rev. Lett. **97**, 135503 (2006).

[15] Y. Nakai, Y. Nakano, T. Azuma, A. Hatakeyama, C. Kondo, K. Komaki, Y. Yamazaki, E. Takada, and T. Murakami, Phys. Rev. Lett. **101**, 113201 (2008).

[16] Y. Nakano, C. Kondo, A. Hatakeyama, Y. Nakai, T. Azuma, K. Komaki, Y. Yamazaki, E. Takada, and T. Murakami, Phys. Rev. Lett. **102**, 085502 (2009).

[17] I. A. Sellin, M. Breinig, W. Brandtc, and R. Laubert, Nucl. Instrum. Methods **194**, 395 (1982).

[18] M. Breinig, S. B. Elston, S. Huldt, L. Liljeby, C. R. Vane, S. D. Berry, G. A. Glass, M. Schauer, I. A. Sellin, G. D. Alton *et al.*, Phys. Rev. A **25**, 3015 (1982).

[19] N. Stolterfoht, Phys. Rep. **146**, 315 (1987).

[20] L. H. Andersen, M. Frost, P. Hvelplund, H. Knudsen, and S. Datz, Phys. Rev. Lett. **52**, 518 (1984).

[21] T. J. M. Zouros, E. P. Benis, M. Zamkov, C. D. Lin, T. G. Lee, P. Richard, T. W. Gorczyca, and T. Morishita, Nucl. Instrum. Methods Phys. Res. B **233**, 161 (2005).

[22] S. Suda, Y. Nakano, K. Metoki, T. Azuma, Y. Takano, A. Hatakeyama, Y. Nakai, K. Komaki, E. Takada, and T. Murakami, Phys. Scr. T **144**, 014044 (2011).